ISBN: 978-3-95450-223-3 ISSN: 2673-7000 doi:10.18429/JACoW-NAPAC2019-MOPLM06

HIGH VOLTAGE DESIGN OF A 350 kV DC PHOTOGUN AT BNL

W. Liu, O. H. Rahman and E. Wang
Brookhaven National Laboratory, Upton, NY 11973, USA

Abstract

Brookhaven National Laboratory is constructing a 350 kV DC high voltage photogun to provide spin-polarized electron beam for the proposed eRHIC facility. The photogun employs a compact inverted-tapered-geometry ceramic insulator that extends into the vacuum chamber and mechanically holds the cathode electrode. By operating at high voltage, the photogun will provide lower beam emittance, thereby improving the beam transmission through the injector apertures, and prolong the operating lifetime of the photogun. However, high voltage increases the field emission, which can result in high voltage breakdown and even lead to irreparable damage of the ceramic insulator. This work describes the methods to minimize the electric field around the metal-vacuum-insulator interface, and to avoid high voltage breakdown and ceramic insulator damage. The triple point junction shields are designed. The simulated electric field, field emission and beam transportation will be presented.

INTRODUCTION

The Electron Ion Collider (EIC) will open a new frontier in nuclear physics, which help to quantitative study the properties of matter from the deeply fundamental Quantum Chromo-Dynamics (QCD) constituents [1]. Brookhaven National Laboratory (BNL) is proposing eRHIC, an electron ion collider based on the existing Relativistic Heavy Ion Collider (RHIC) facility with an additional electron storage ring [2]. The eRHIC requires a direct current (DC) high voltage photoemission electron gun (photogun) to generate spin-polarized electron beam by illuminating a strained superlattice GaAs photocathode with circularly polarized light. The polarized electron beams is injected into the electron storage ring for collision with the polarized protons or heavy ions of RHIC. In the eRHIC design, the polarized electron injector need to provide high current and high bunch charge. A photogun, aimed to provide electron beam with 10 mA average current and 5.3 nC bunch charge, is under development at BNL [3].

In this paper, we report on the high voltage design of the 350 kV DC photogun with the compact "inverted" insulator structure, which can provide smaller volume and less surface area to contribute a gas load, resulting in better achievable vacuum. The photogun also has less metal that was biased at high voltage and contributed to field emission, due to the insulator serves as the cathode electrode support structure, compared to the "standard" photogun that applied the metal stalk to hold the cathode electrode. A triple-point-junction shield (TPJS) was attached together with the cathode electrode to reduce the electric field around the metal-vacuum-insulator interface (triple point junction) to eliminate the field emission from this junction, and to avoid the damage of insulator. Design and optimization of the TPJS structure will be described. The affects to the electron beam by introducing the TPJS will also be present.

HIGH VOLTAGE STRUCTURE DESIGN

Figure 1 shows the 3D model of the DC high voltage photogun with its major components. This photogun applied the inverted-tapered-geometry ceramic insulator structure that extends into the spherical vacuum chamber (91.44 cm diameter) and mechanically holds the spherical cathode electrode (20 cm diameter). The cathode electrode was manufactured by welding two hydroformed hemisphere stainless steel shells and was polished by mechanical polishing to obtain a exceptionally smooth surface. An internal fixture was installed in the spherical electrode, which serves to fix the electrode to the insulator and also to hold the photocathode puck. The high voltage cable (0.5 cm diameter) was covered with vulcanized rubber plug and was placed inside the hollow ceramic insulator. One end of the cable was connected to the endpoint of the ceramic insulator, where a stainless steel bulk was tightly mechanically jointed to the insulator by Kovar (nickel-cobalt ferrous alloy) that is a good insulator-to-metal seal material. Another end of the cable was connected to a high voltage power supply that can provide a voltage up to 400 kV.

The "inverted" photogun has been successfully operated at 100-200 kV, and recently test the photogun at 350 kV at JLab [4–6]. However, breakdown and puncher often hap-

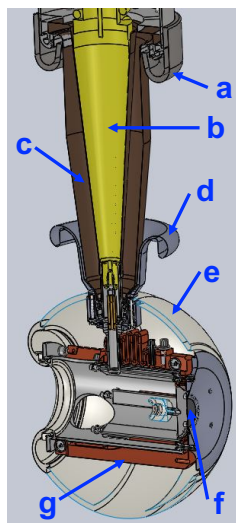

Figure 1: The 3D model of the high voltage structure, a) ground TPJS, b) ceramic insulator, c) rubber cable plug, d) HV TPJS, e) cathode electrode, f) photocathode sample, g) internal fixture.

ISBN: 978-3-95450-223-3 ISSN: 2673-7000 doi:10.18429/JACoW-NAPAC2019-MOPLM06

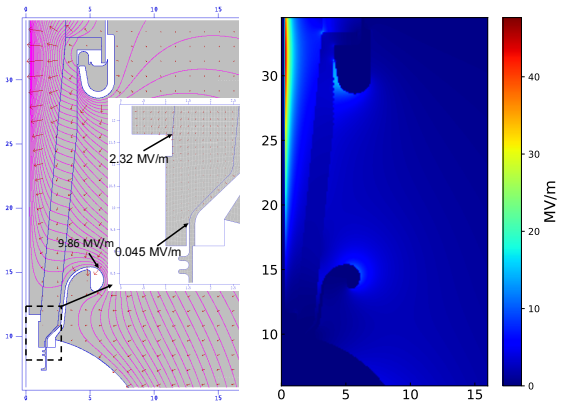

Figure 2: Electric field maps at 400 kV modeled with field solver program Poisson Superfish for the HV structure with triple-point-junction shield.

pen when the voltage on the cathode reached above 300 kV. Two methods have been used to avoid the breakdown and puncher: reducing the resistivity of insulator by coating with conductive film on the insulator surface or doping the insulator, adding the triple-point-junction shield at the high voltage end of insulator(called HV TPJS) to eliminate the field emission from the metal-vacuum-insulator interface. However, until now, breakdown and puncher near the ground end of insulator still happen sometimes. A TPJS was placed at the ground end of insulator (called Ground TPJS) in our photogun to optimize the potential gradient along the insulator near the ground end, due to the linear potential helps to avoid breakdown [7]. A HV TPJS was also installed, which was carefully optimized to reduce the field emission from the HV TPJS, leading to the field emitted electrons that reached to the insulator surface was as few as possible.

SIMULATED RESULTS

To estimate the electric field strength and optimize the shape of triple-point-junction shield, the static electric field was modeled using the Poisson Superfish. The vulcanized rubber plug was modeled as a material with dielectric constant ($\varepsilon_r = \varepsilon_1/\varepsilon_0$) of 2.37. The ceramic insulator was set as 94.7% alumina (a doped insulator) with dielectric constant of 8.4. The other structures were modeled as high voltage or ground metal. The modeled electric field maps are shown in Fig. 2, in which the voltage was set to 400 kV. The equipotential lines are shown in pink color. Field arrows are shown in red color. The blue lines represent the boundary of the structures.

According to the Fowler-Nordheim equation [8], higher electric field on the metal surface contributes to an increased emission of electrons. The localized electric field near the micro-protrusions and particulate contamination on the metal surface was enhanced and more easily generated field emission. The smoothness of metal surface determine the threshold of field emission. And more smooth on the metal surface, higher field emission threshold. To see how the field

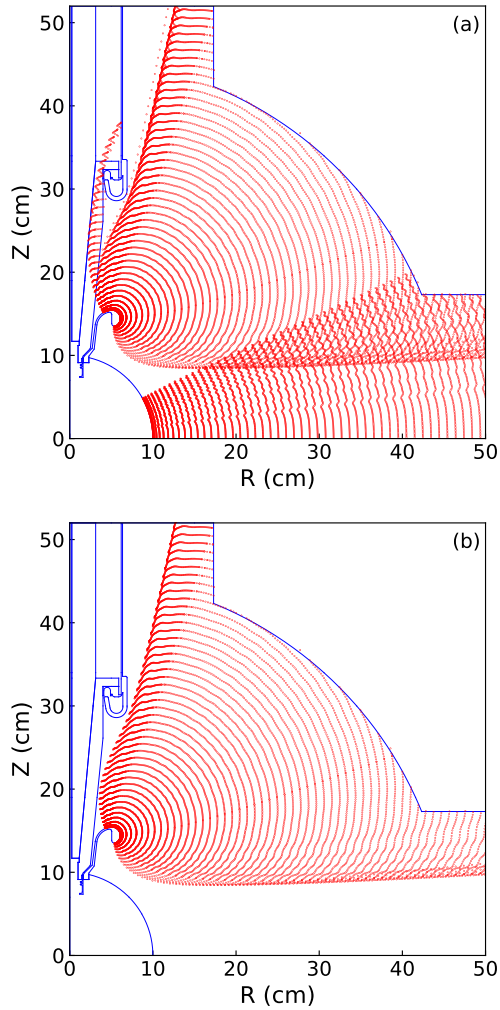

Figure 3: The trajectories of field emitted electrons for field emission threshold of (a) 4.5 MV/m and (b) 5 MV/m

emitted electrons move in the photogun, the field emission was tracked using Python code. The code firstly loads the electric field map and mesh the field map, then set electrons emitted from the metal surface where the field strength is higher than the field emission threshold and the voltage is −400 kV. Finally, these electrons move in each mesh of field map where electrons located in, and iterate the moving of electrons until they stopped at the ground surface. The calculated trajectories of field emitted electrons for field emission threshold of 4.5 MV/m and 5 MV/m is shown in Fig. 3. There are some field emitted electrons that will strike on the insulator when the field emission threshold was 4.5 MV/m. However, no electrons will strike on the insulator when the field emission threshold was 5 MV/m, which means the breakdown and puncher will not happen. The field emission threshold of polished stainless steel is typically higher than 8 MV/m [9]. Thus, the field emitted electrons generated from the polished TPJS would not strike on the insulator, avoiding the breakdown and puncher.

ISBN: 978-3-95450-223-3 ISSN: 2673-7000 doi:10.18429/JACoW-NAPAC2019-MOPLM06

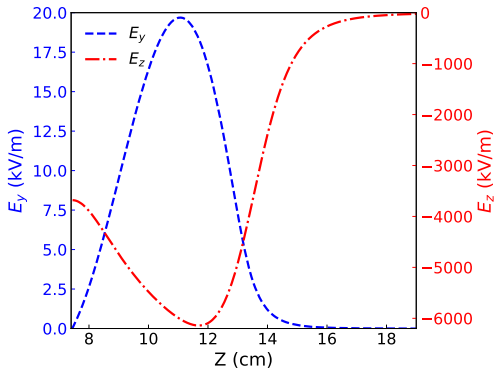

Figure 4: The transverse (E_y) and longitudinal (E_z) electric field strength along the center line (Z axis) within the cathode-anode gap. The bias voltage is 350 kV.

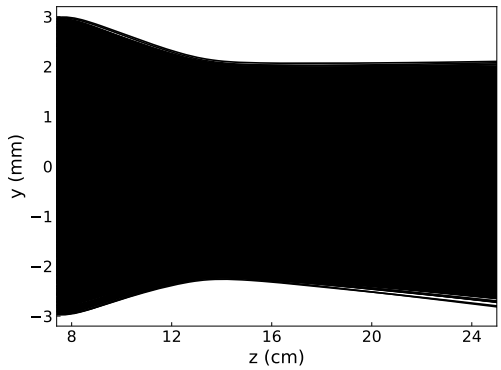

Figure 5: The trajectory of electron beam emitted from photocathode within the cathode-anode gap with the gap distance of 5.7 cm.

The high voltage structure destroyed the symmetry of the electric field within cathode-anode gap. The TPJS contributed to increase the asymmetry of the electric field within the cathode-anode gap, which introduced the transverse electric field along the center line within the cathode-anode gap. For symmetric cathode-anode design, the transverse electric field along the center line is zero. Under the influence of this transverse electric field, the photo-electron beam will be deflected within the cathode-anode gap, called "transverse kick" to the electron beam. Maintaining an acceptable value of the transverse kick is another key factor during optimizing the structure of TPJS.

Opera Simulation Software was used to simulate the electric field within the cathode-anode gap, because the Poisson Superfish is not suited for calculating the electric field of asymmetric structure. Figure 4 shows the transverse and longitudinal electric field strength along the center line within the cathode-anode gap. The longitudinal electric field contributes to accelerate the electron beam emitted from the photocathode, and the transverse electric field contributes to deflect the electron beam. The maximum transverse electric field strength is only 0.3% of the maximum longitudinal electric field strength. The ratio of transverse to longitudinal electric field strength directly determine the deflection distance of electron beam.

To better estimate the effect of the transverse electric field on the electron beam quality, electron beam trajectory simulation was performed using the 3D particle tracking simulation code General Particle Tracer (GPT), in which the space charge effect was included. The simulated trajectory of electron beam within the cathode-anode gap is shown in Fig. 5. In the simulation, the electron beam is set to be uniform with diameter of 6 mm; the intrinsic thermal emittance is 0.77 mm-mrad; the electron bunch length is 1.5 ns and the electron bunch charge is 5.3 nC. Obviously, the electron beam is deflected in the y direction under the influence of transverse electric field. The deflection distance is 0.072 mm at the anode position (z=13.1 cm). And the deflection distance is 0.288 mm at z=22 cm, where an offset kicker will be placed to deflect electron beam back to the center line within the beam pipe. The deflection distance is <5% of the beam size, and is acceptable for our photogun.

CONCLUSIONS AND FUTURE WORK

The electric field at metal-vacuum-insulator interface was significantly eliminate by applying triple point shield, which will effectively suppress the field emission at the interface. The triple point shield structure was also optimized to prevent the field emitted electrons striking the insulator to avoid the HV breakdown and puncher. The transverse electric field within the cathode-anode gap was minimized by optimizing the HV structures. The corresponding transverse kick to the electron beam is very small compared to the beam size.

REFERENCES

[1] A. Accardi, *et al.*, "Electron-Ion Collider: The next QCD frontier," *Eur. Phys. J. A*, vol. 52, p. 268, 2016. doi:10.1140/epja/i2016-16268-9; arXiv:1212.1701, 2014.

[2] E. C. Aschenauer, *et al.*, "eRHIC Design Study: An Electron-Ion Collider at BNL," https://arxiv.org/abs/1409.1633, 2014.

[3] E. Wang, "High current polarized electron source for future eRHIC," *AIP Conf. Proc.*, vol. 1970, p. 050008, 2018. doi:10.1063/1.5040227

[4] C. Hernandez-Garcia, D. Bullard, F. Hannon, Y. Wang, and M. Poelker, "High voltage performance of a dc photoemission electron gun with centrifugal barrel-polished electrodes," *Rev. Sci. Instrum.*, vol. 88, p. 093303, 2017. doi:10.1063/1.4994794

[5] C. Hernandez-Garcia, M. Poelker, and J. Hansknecht, "High voltage studies of inverted-geometry ceramic insulators for a 350 kV DC polarized electron gun," *IEEE Trans. Dielectr. Electr. Insul.*, vol. 23, p. 418, 2016. doi:10.1109/TDEI.2015.005126

[6] G. Palacios-Serrano, F. Hannon, C. Hernandez-Garcia, M. Poelker, and H. Baumgart, "Electrostatic design and conditioning of a triple point junction shield for a -200 kV DC high voltage photogun," *Rev. Sci. Instrum.*, vol. 89, p. 104703, 2018. doi:10.1063/1.5048700

ISBN: 978-3-95450-223-3 ISSN: 2673-7000 doi:10.18429/JACoW-NAPAC2019-MOPLM06

[7] A.S. Pillai and R. Hackam, "Modification of electric field at the solid insulator-vacuum interface arising from surface charges on the solid insulator," *J. Appl. Phys.*, vol. 54, p. 1302, 1983. doi:10.1063/1.332204

[8] A.V. Crewe, D. N. Eggenbbrger, J. Wall, and L. M. Welter, "Electron Gun Using a Field Emission Source," *Rev. Sci. Instrum.*, vol. 39, p. 576, 1968. doi:10.1063/1.1683435

[9] M. Bastaninejad, *et al.*, "Evaluation of electropolished stainless steel electrodes for use in DC high voltage photoelectron guns," *J. Vac. Sci. Technol. A*, vol. 33, p. 041401, 2015. doi:10.1116/1.4920984